

Strong deflection of massive particles in spherically symmetric spacetimes

Fabiano Feleppa,^{1,2,*} Valerio Bozza,^{1,2,†} and Oleg Yu. Tsupko^{3,4,‡}

¹*Dipartimento di Fisica “E.R. Caianiello”, Università di Salerno,
Via Giovanni Paolo II 132, I-84084 Fisciano, Italy*

²*Istituto Nazionale di Fisica Nucleare, Sezione di Napoli, Via Cintia, 80126, Napoli, Italy*

³*ZARM, University of Bremen, 28359 Bremen, Germany*

⁴*Institut für Theoretische Physik, Goethe Universität, Max-von-Laue-Strasse 1, 60438 Frankfurt, Germany*

Near a gravitating compact object, massive particles traveling along timelike geodesics are gravitationally deflected similarly to light. In this paper, we study the deflection angles of these particles in the strong deflection limit. This analytical approximation applies when particles in unbound orbits approach the compact object very closely, circle around it at a radius close to that of the unstable circular orbit, and eventually escape. While previous studies have provided results for particular metrics, we offer a general solution applicable to any static, spherically symmetric and asymptotically flat spacetime. After briefly reviewing the exact expression for the deflection angle of massive particles, we present a strong deflection limit analysis for this general case. The developed formulas are then applied to three particular metrics: Schwarzschild, Reissner-Nordström and Janis-Newman-Winicour.

Keywords: strong deflection limit; massive particles; black holes

I. INTRODUCTION

The deflection of particles by gravity is primarily studied in the case of light rays. Measuring the deflection of starlight during a total solar eclipse provided the first experimental proof of general relativity. Since then, gravitational lensing has become a crucial tool in astrophysics, allowing one to investigate a wide range of phenomena. In most observational scenarios, the bending of light by gravity is very small. Therefore, the well-known Einstein formula for the deflection angle, which assumes a weak deflection, is usually sufficient for describing these lensing events.

On the other hand, the groundbreaking imaging of the supermassive black hole in M87 [1–6] and the black hole at the center of our Galaxy [7–12] have marked the beginning of a new chapter in the study of gravitational lensing, opening up possibilities to test general relativity beyond the weak deflection limit. When light rays are deflected by extremely compact gravitating objects, the bending can indeed become significant. Theoretical studies on the deflection of light by compact objects have also a long history. In 1959, Darwin [13] studied the motion of particles in a Schwarzschild spacetime. Notably, he developed a logarithmic approximation, now known as the strong deflection limit, to describe the deflection of light rays moving near the photon sphere — the boundary encompassing all unstable circular orbits of photons with any possible inclinations. The strong deflection limit analysis proposed by Darwin was much later generalized to any spherically symmetric solution to Einstein field equations in Ref. [14], as well as to axisymmetric solutions [15]. Over the years, a multitude of both analytical

and numerical studies extending beyond the weak deflection limit approximation have been published (see, e.g., Refs. [16–52]). Additionally, several recent studies have focused on higher-order images specifically in the form of photon rings (see, e.g., Refs. [53–68]).

Analogous to photons, massive particles are also deflected in the presence of a gravitational field. The motion of massive test particles in black hole-like spacetimes has a long history as well [13, 18, 69–82]. Over the past two decades, numerous works have also focused on calculating the deflection angle of massive particles by compact objects. In 2002, the deflection angle of relativistic, massive particles propagating in a Schwarzschild spacetime was calculated up to the second post-Newtonian order [83]. In 2014, a strong deflection limit analysis for massive particles in Schwarzschild spacetime was presented for the first time [84]. Two years later, the same scenario has been considered in Ref. [85], with more emphasis on possible applications. In 2018, the Gauss-Bonnet theorem was applied to derive the deflection angle in the Schwarzschild metric up to second post-Newtonian order [86], using a method developed by Gibbons and Werner [87]; see also Ref. [88], where this method is extensively applied. In 2019, the deflection angle calculation was extended to the Reissner-Nordström spacetime, considering both weak and strong deflection approximations [89]. In 2020, the deflection for massive particles in the Schwarzschild-de Sitter metric was derived up to the second post-Newtonian order [90]. Most recently, an analytically exact treatment of the gravitational lensing of massive particles in the charged Newman-Unti-Tamburino metric was presented by Frost [91]. For a discussion on the black hole shadows of massive particles, the reader may refer to Refs. [92, 93]; see also Refs. [94, 95]. For exact calculations of timelike and null geodesics using various special functions, the reader may consult Refs. [32, 33, 49, 50].

Quite surprisingly, a strong deflection limit analysis

* Correspondence email address: ffeleppa@unisa.it

† Correspondence email address: vbozza@unisa.it

‡ Correspondence email address: tsupkooleg@gmail.com

for massive particles that applies to any static, asymptotically flat and spherically symmetric spacetime is still missing. In this paper, our goal is to fill this gap, following the procedure outlined in Ref. [14]. Specifically, to write the general formulas, we apply the results from Sec. III of Ref. [96], where a strong deflection limit analysis for photons propagating in a spherically symmetric spacetime surrounded by plasma is discussed. The connection between the two physically different scenarios — the one discussed here and the other in Ref. [96] — can be understood by noting that a photon wave packet in homogeneous plasma behaves like a massive particle with a velocity equal to the group velocity of the wave packet, a rest mass equal to the plasma frequency and an energy equal to the photon energy, see Refs. [97–99] for details.

We can consider several scenarios in which our formulas could be applied. One such scenario is the gravitational deflection of massive particles. If a distant source emits massive particles, they can be deflected by a gravitating body, forming multiple images and exhibiting other effects analogous to light lensing. For a detailed discussion, see Frost [91]. Since the focus here is on neutral particles (where electromagnetic interaction is not involved), neutrinos are the primary candidates for this consideration. For instance, neutrinos emitted by supernovae [100] can experience strong deflection when passing near black holes [101]. The lensing of neutrinos specifically has been studied in works such as [101–107]. Typically, neutrinos are approximated as massless particles, and lensing effects are calculated using formulas originally derived for light rays. For example, Eiroa and Romero [102] investigated the deflection of neutrinos by very compact objects, applying bending angle formulas intended for light. Although neutrinos travel at velocities very close to the speed of light, the bending angles for massless and massive particles are, in principle, different.

A second scenario for applying our formulas is in the study of extreme mass ratio inspirals (EMRIs), where a compact object, such as a stellar-mass black hole or neutron star, orbits a supermassive black hole. For a more detailed discussion, the reader is referred to Ref. [84]. EMRIs are sources of gravitational waves and are a primary target for the planned Laser Interferometer Space Antenna (LISA) mission [108–110]. Of particular interest in this context are studies of pulsars in close orbits around supermassive black holes [111, 112].

The paper is organized as follows. In Sec. II, we consider the unbound motion of a massive test particle in a static, spherically symmetric and asymptotically flat spacetime, and derive the well-known exact expression for the deflection angle of such a particle in terms of its energy per unit rest mass. In Sec. III, we obtain the equation from which the radial coordinate of unstable circular orbits of massive particles can be deduced. In Sec. IV, starting from the exact expression for the deflection angle derived in Sec. II, we present a strong deflection limit analysis. The general formulas from Sec. IV are then applied to three particular cases: the Schwarzschild met-

ric, the Reissner-Nordström metric and finally the Janis-Newman-Winicour metric, see Sec. V). We conclude, in Sec. VI, with a summary of the results obtained.

In what follows, we set $G = c = 1$ and use the signature convention $\{-, +, +, +\}$. Moreover, we will work in Schwarzschild coordinates (t, r, θ, φ) . Greek indices sum over these coordinates.

II. DEFLECTION ANGLE OF MASSIVE PARTICLES IN STATIC AND SPHERICALLY SYMMETRIC SPACETIMES

Let us consider an unbound orbit of a massive particle moving from infinity towards a very compact central object, bending its trajectory, reaching a minimum radial coordinate (also referred to as “closest approach distance”), say r_0 , and then going to infinity again. Restricting our attention to the case of a lensing object described by a static, spherically symmetric and asymptotically flat spacetime, we will now derive an exact expression for the deflection angle of the particle, in integral form. We will follow and generalize the derivation from Refs. [18, 77], where the Schwarzschild metric was considered. See also Refs. [75, 113].

The equations governing the geodesics in a spacetime with the line element

$$ds^2 = g_{\mu\nu} dx^\mu dx^\nu \quad (1)$$

can be derived from the Lagrangian

$$\mathcal{L} = \frac{1}{2} g_{\mu\nu} \frac{dx^\mu}{d\tau} \frac{dx^\nu}{d\tau}, \quad (2)$$

where τ is some affine parameter along the geodesic. For timelike geodesics, τ may be identified with the proper time of the particle.

The line element describing the class of spacetimes under investigation can be written as

$$ds^2 = g_{\mu\nu} dx^\mu dx^\nu = -A(r) dt^2 + B(r) dr^2 + C(r) d\Omega^2, \quad (3)$$

where $d\Omega^2 := d\theta^2 + \sin^2\theta d\varphi^2$ defines the round metric on the unit two-sphere. As anticipated, we assume the spacetime to be asymptotically flat, so the metric coefficients $A(r)$, $B(r)$ and $C(r)$ satisfy

$$\lim_{r \rightarrow \infty} A(r) = 1, \quad \lim_{r \rightarrow \infty} B(r) = 1, \quad \lim_{r \rightarrow \infty} C(r) = r^2. \quad (4)$$

The metric coefficients are positive in the asymptotically flat region. Approaching the origin, some of them may change sign; we denote the interval in which all the metric coefficients are strictly positive as $\tilde{r} < r < \infty$ (in the case of black holes, such interval extends from the radius of the event horizon to infinity).

The Lagrangian (2), specialized to our case, becomes

$$\mathcal{L} = \frac{1}{2} [-A(r)\dot{t}^2 + B(r)\dot{r}^2 + C(r)\dot{\varphi}^2], \quad (5)$$

where, without loss of generality, we considered the orbit of our particle to be confined to the equatorial plane (i.e., we set $\theta = \pi/2$). In the above expression, the dot denotes differentiation with respect to the proper time τ . Now, the equation of motion for \dot{t} gives

$$\frac{\partial \mathcal{L}}{\partial t} - \frac{d}{d\tau} \frac{\partial \mathcal{L}}{\partial \dot{t}} = 0 \Rightarrow \dot{t} = \frac{E}{A(r)}, \quad E = \text{constant}, \quad (6)$$

while the one for $\dot{\varphi}$ leads to

$$\frac{\partial \mathcal{L}}{\partial \varphi} - \frac{d}{d\tau} \frac{\partial \mathcal{L}}{\partial \dot{\varphi}} = 0 \Rightarrow \dot{\varphi} = \frac{L}{C(r)}, \quad L = \text{constant}. \quad (7)$$

In an asymptotically flat spacetime, as the one we are considering, the constant E represents the energy at infinity per unit rest mass of the particle, while the constant L is the angular momentum per unit rest mass of the particle. From the condition $2\mathcal{L} = -1$, that is,

$$g_{\mu\nu} \frac{dx^\mu}{d\tau} \frac{dx^\nu}{d\tau} = -1, \quad (8)$$

we can immediately derive an equation for \dot{r} , given by

$$-A(r)\dot{t}^2 + B(r)\dot{r}^2 + C(r)\dot{\varphi}^2 = -1. \quad (9)$$

The above equation can be also rewritten as

$$\dot{r}^2 + \frac{1}{B(r)} \left(1 + \frac{L^2}{C(r)} \right) = \frac{E^2}{A(r)B(r)}. \quad (10)$$

By combining Eqs. (7) and (10), the orbit equation of the particle can be easily derived as

$$\begin{aligned} \frac{d\varphi}{dr} &= \pm \frac{L}{C(r)} \frac{1}{\sqrt{\frac{E^2}{A(r)B(r)} - \frac{1}{B(r)} \left(1 + \frac{L^2}{C(r)} \right)}} \\ &= \pm \frac{1}{C(r)} \frac{\sqrt{B(r)}}{\sqrt{\frac{1}{L^2} \left(\frac{E^2}{A(r)} - 1 \right) - \frac{1}{C(r)}}}. \end{aligned} \quad (11)$$

Suppose the test particle moves such that its angular coordinate φ increases. In this case, the positive sign in the above equation indicates motion where the coordinate r is also increasing, while the negative sign corresponds to motion where r decreases.

Eq. (11) can be compared, for example, with Eq. (102) of Ref. [86]. The case $C(r) = r^2$ was also considered in Ref. [75].

By imposing that $dr/d\varphi$ vanishes at r_0 , we obtain a simple relation between L and the distance of closest approach r_0 , namely

$$L^2 = C(r_0) \left(\frac{E^2}{A(r_0)} - 1 \right). \quad (12)$$

Unlike the trajectories of light rays, which are determined by a single parameter (typically the closest approach distance or the impact parameter), the trajectories of massive particles in this spacetime depend on two parameters. For the equation (11), these parameters are E and

L . Since the closest approach distance r_0 will appear as an integration limit in the formula for the deflection angle (see below), it is convenient to eliminate another variable, either E or L , using Eq. (12). This allows us to express the equations in terms of either the pair (r_0, E) or the pair (r_0, L) ; see Ref. [84].

Substituting Eq. (12) into Eq. (11), we can write

$$\frac{d\varphi}{dr} = \pm \sqrt{\frac{B(r)}{C(r)}} \left[\frac{C(r)A(r_0)}{C(r_0)A(r)} \frac{1 - \frac{A(r)}{E^2}}{1 - \frac{A(r_0)}{E^2}} - 1 \right]^{-1/2}. \quad (13)$$

Above, we present the right-hand side of the orbit equation in terms of r_0 and E . As discussed earlier, by using Eq. (12), we could also express it in terms of r_0 and the angular momentum L . However, in this article, we will focus exclusively on the (r_0, E) pair for two reasons. First, the energy at infinity, E , is directly related to the velocity at infinity, which is a very convenient parameter for applications. Second, expressing formulas in terms of E allows us to take advantage of the equivalence between the motion of massive particles in a vacuum and the motion of photons in a homogeneous plasma discussed in our previous paper [96]. Indeed, it is immediate to notice the mathematical equivalence between Eq. (13) and the radicand of Eq. (9) in Ref. [96] specialized to the case of homogeneous plasma. More specifically, we notice that the quantity $1 - A(r)/E^2$ appearing in Eq. (13) can be thought of as the homogeneous plasma refractive index, provided that we identify $E^{-2} \leftrightarrow \omega_e^2/\omega_\infty^2$, where ω_e represents the plasma frequency (constant in the homogeneous case) and ω_∞ the photon frequency measured by an observer at infinity.

As already anticipated in Sec. I, all the formulas obtained in Sec. IV A of Ref. [96] can be applied to the present case, by simply considering the replacement above.

In order to simplify the notation, we will adopt the subscript 0 when a quantity is evaluated at r_0 . Furthermore, we define

$$\mathcal{F}^2(r, E) := 1 - \frac{A(r)}{E^2}. \quad (14)$$

Eq. (13) can then be rewritten as

$$\frac{d\varphi}{dr} = \pm \sqrt{\frac{B(r)}{C(r)}} \left(\frac{C(r)}{C_0} \frac{A_0}{A(r)} \frac{\mathcal{F}^2(r, E)}{\mathcal{F}_0^2} - 1 \right)^{-1/2}. \quad (15)$$

If we now assume that particles travel in such a way that their angular coordinate φ increases, then we must choose the positive sign in Eq. (13) when the coordinate r is also increasing; conversely, the negative sign is chosen when the coordinate r is decreasing. Therefore, for a particle coming from infinity towards the gravitational object, and then going to infinity again, the change in the angular coordinate φ reads

$$\Delta\varphi = 2 \int_{r_0}^{\infty} \frac{\sqrt{B}}{\sqrt{C} \sqrt{\frac{C}{C_0} \frac{A_0}{A} \frac{\mathcal{F}^2}{\mathcal{F}_0^2} - 1}} dr, \quad (16)$$

where, for simplicity, we omitted the dependencies of the various quantities. If the trajectory were a straight line, $\Delta\varphi$ would equal just π . Thus, we obtain the deflection angle of the particle with energy at infinity E travelling from infinity towards the compact body, reaching a minimum distance r_0 , and then to infinity again, as

$$\hat{\alpha}(r_0, E) = 2 \int_{r_0}^{\infty} \frac{\sqrt{B}}{\sqrt{C} \sqrt{\frac{C}{C_0} \frac{A_0}{A} \frac{\mathcal{F}^2}{\mathcal{F}_0^2} - 1}} dr - \pi. \quad (17)$$

In this formula, the coefficients A , B , and C depend only on r , while the function \mathcal{F} , defined in (14), depends on both r and E . Additionally, we note that the deflection angle of light rays is recovered in the limit $E \rightarrow \infty$. In this case, both $\mathcal{F} \rightarrow 1$ and $\mathcal{F}_0 \rightarrow 1$. For comparison, see, for example, Refs. [75, 114].

Our goal is to find an analytical approximation of the deflection angle (17) in the strong deflection limit. Analogous to the behavior of photons, when r_0 approaches the radius of the particle's unstable circular orbit (r_c), the particle will orbit the black hole several times before finally escaping. The case $r_0 = r_c$ corresponds to particles that fall directly onto the unstable circular orbit, at which point the deflection angle diverges (see Sec. IV).

Exploiting the mathematical analogy between photons traveling in homogeneous plasma and massive particles mentioned above, it becomes clear that all the general results presented in Ref. [96] can be applied to the present case with only minor adjustments.

III. UNSTABLE CIRCULAR ORBITS OF MASSIVE PARTICLES

Before proceeding, let us first derive the equation from which one can deduce the radius of the unstable circular orbit of the massive particle once the metric coefficients are specified. As we will see, such equation will depend on E or L and will be valid only in a certain range of these parameters. To do so, let us go back to Eq. (10), which can be recast in the form

$$\dot{r}^2 = \frac{1}{B(r)} \left(\frac{E^2}{A(r)} - \frac{L^2}{C(r)} - 1 \right). \quad (18)$$

The particle follows a circular motion if, at a fixed radius $r = r_*$, the following two conditions are satisfied:

$$\left. \frac{dr}{d\tau} \right|_{r=r_*} = 0, \quad (19)$$

$$\left. \frac{d^2r}{d\tau^2} \right|_{r=r_*} = 0. \quad (20)$$

The first of the above conditions immediately leads to

$$L^2 = C(r_*) \left(\frac{E^2}{A(r_*)} - 1 \right). \quad (21)$$

Now, differentiating Eq. (18) with respect to τ and dividing by \dot{r} , gives [115]

$$2\ddot{r} = \frac{d}{dr} \left[\frac{1}{B(r)} \left(\frac{E^2}{A(r)} - \frac{L^2}{C(r)} - 1 \right) \right]. \quad (22)$$

Therefore, Eq. (20) reduces to the requirement

$$\left. \frac{d}{dr} \left[\frac{1}{B(r)} \left(\frac{E^2}{A(r)} - \frac{L^2}{C(r)} - 1 \right) \right] \right|_{r=r_*} = 0. \quad (23)$$

By using Eq. (21), we can write the above expression in terms of E , resulting in

$$\frac{C'(r_*)}{C(r_*)} - \frac{A'(r_*)}{A(r_*)} \left(1 - \frac{A(r_*)}{E^2} \right)^{-1} = 0. \quad (24)$$

The above expression can be compared, for example, with Eq. (30) in Ref. [116]. Let us assume that Eq. (24) admits at least one positive solution which reduces, in the limit $E \rightarrow \infty$, to the radius of the photon sphere. Such a solution corresponds to the radius of the unstable circular orbit of the massive particle and will be valid, as already mentioned, within a certain range of values of E .

As a consistency check, let us now consider Eq. (24) in the case of a Schwarzschild black hole. By defining the Schwarzschild radius $r_S = 2M$ ($G = c = 1$) as the unit of measure of distances, with M being the mass of the black hole, the metric coefficients can be written as

$$A(r) = 1 - \frac{1}{r}, \quad (25)$$

$$B(r) = \left(1 - \frac{1}{r} \right)^{-1}, \quad (26)$$

$$C(r) = r^2. \quad (27)$$

The solution of Eq. (24) is

$$r_c = r_c(E) = \frac{3E^2 - 4 + E\sqrt{9E^2 - 8}}{4(E^2 - 1)}, \quad (28)$$

as expected [84]. In the limit $E \rightarrow \infty$, r_c reduces to $3/2$ (radius of the photon sphere, see Ref. [14]). Now, by introducing the variable

$$x = x(E) := \sqrt{1 - \frac{8}{9E^2}}, \quad (29)$$

Eq. (28) can be rewritten as [84]

$$r_c = r_c(x) = 3 \frac{1+x}{1+3x}. \quad (30)$$

From Eq. (29), we deduce that $E \geq \sqrt{8}/3$, which corresponds to the energy of a particle in the innermost stable circular orbit (in units of $2M$, the radius of the innermost stable circular orbit is equal to 3); according to Eq. (30), r_c then varies from 3 to $3/2$ if the energy E varies from $\sqrt{8}/3$ to infinity. However, as we can easily deduce from Eq. (18), we must impose that $E \geq 1$ in order to allow the particle to escape to $r = \infty$. Thus, the allowed range of E is $[1, \infty)$.

IV. DEFLECTION ANGLE IN THE STRONG DEFLECTION LIMIT

We are now ready to perform a strong deflection limit analysis on Eq. (17). In this section, we extend the procedure originally proposed in Ref. [14], which applies to light rays that come close to the photon sphere, to the case of massive particles.

With decreasing r_0 (the distance of closest approach), the deflection angle increases, causing the particle to circle the compact object several times before escaping. As r_0 approaches r_c , the radius of the particle's unstable circular orbit, the deflection angle approaches infinity.

As already mentioned, we can directly apply all the results from Ref. [96] to the present case. Most of the formulas in this section are, in fact, obtained from the ones in [96] by appropriately substituting variables and adjusting notation. Nevertheless, while the core methodology remains unchanged, it is important to provide a brief overview of the procedure's steps here in order to clarify the results, approximations and assumptions that are used in this paper. This includes addressing any modifications to the original framework that are necessary for the current application, as well as providing detailed explanations of the particular cases and scenarios that are discussed in the following sections.

We introduce the variable z as

$$z = \frac{A(r) - A_0}{1 - A_0}. \quad (31)$$

Consequently, we have

$$r = A^{-1}[A_0 + (1 - A_0)z], \quad (32)$$

where A^{-1} denotes the inverse function and the expression in square brackets is its argument. The deflection angle, Eq. (17), can then be rewritten as

$$\hat{\alpha}(r_0, E) = I(r_0, E) - \pi, \quad (33)$$

$$I(r_0, E) := \int_0^1 R(z, r_0, E) f(z, r_0, E) dz, \quad (34)$$

$$R(z, r_0, E) := \frac{2\mathcal{F}_0 \sqrt{ABC_0}(1 - A_0)}{CA'}, \quad (35)$$

$$f(z, r_0, E) := \frac{1}{\sqrt{A_0 \mathcal{F}^2 - [(1 - A_0)z + A_0] \frac{C_0}{C} \mathcal{F}_0^2}}. \quad (36)$$

According to Eq. (32), any quantity without the subscript 0 is evaluated at r . In line with Refs. [14, 96], we approximate $f(z, r_0, E)$ to second order in z , and define

$$f_0(z, r_0, E) := \frac{1}{\sqrt{\alpha z + \beta z^2}}, \quad (37)$$

with $\alpha = \alpha(r_0, E)$ given by

$$\alpha := \frac{\mathcal{F}_0^2(1 - A_0)}{C_0 A_0'} \left[C_0' A_0 + C_0 \left(2A_0 \frac{\mathcal{F}_0'}{\mathcal{F}_0} - A_0' \right) \right], \quad (38)$$

and $\beta = \beta(r_0, E)$ expressed as

$$\begin{aligned} \beta := & \frac{\mathcal{F}_0^2(1 - A_0)^2}{2C_0^2 A_0'^3} \left[2C_0 C_0' A_0'^2 \right. \\ & + A_0' A_0 (C_0 C_0'' - 2C_0'^2) \\ & \left. - C_0^2 A_0'' A_0 \left(\frac{C_0'}{C_0} + 2 \frac{\mathcal{F}_0'}{\mathcal{F}_0} \right) \right] \\ & + \frac{A_0(1 - A_0)^2}{A_0'^2} (\mathcal{F}_0'^2 + \mathcal{F}_0 \mathcal{F}_0''). \end{aligned} \quad (39)$$

To examine paths that approach r_c , we define a parameter $\delta \ll 1$ as follows:

$$r_0 := r_c(1 + \delta). \quad (40)$$

Note that r_c depends on E , see Eqs. (30) and (29).

We also notice that, setting $\alpha = 0$, gives the radius of the particle's unstable circular orbit. Indeed, we have

$$\alpha = 0 \Rightarrow C_0' A_0 - C_0 A_0' = -2C_0 A_0 \frac{\mathcal{F}_0'}{\mathcal{F}_0}. \quad (41)$$

Now, recalling the definition of \mathcal{F} , Eq. (14), we obtain

$$\frac{\mathcal{F}_0'}{\mathcal{F}_0} = -\frac{A_0'}{2(E^2 - A_0)}, \quad (42)$$

which, substituted into Eq. (41), leads to

$$\frac{C_0'}{C_0} - \frac{A_0'}{A_0} \left(1 - \frac{A_0}{E^2} \right)^{-1} = 0. \quad (43)$$

Eq. (43) coincides with Eq. (24) derived in Sec. III.

By introducing the function

$$g(z, r_0, E) := R(z, r_0, E) f(z, r_0, E) - R(0, r_c, E) f_0(z, r_0, E), \quad (44)$$

Eq. (34) can be split into two parts, namely

$$I(r_0, E) = I_D(r_0, E) + I_R(r_0, E), \quad (45)$$

$$I_D(r_0, E) := \int_0^1 R(0, r_c, E) f_0(z, r_0, E) dz, \quad (46)$$

$$I_R(r_0, E) := \int_0^1 g(z, r_0, E) dz. \quad (47)$$

The subscript D stands for ‘‘divergent’’ (since I_D indeed diverges in the limit $r_0 \rightarrow r_c$), while the subscript R stands for ‘‘regular’’. By explicitly calculating $I_D(r_0, E)$ and subsequently expanding the coefficient α up to first order in δ , we obtain

$$I_D(r_0, E) \simeq -a \log \delta(r_0) + b_D + \mathcal{O}(\delta), \quad (48)$$

where we define

$$a := \frac{R(0, r_c, E)}{\sqrt{\beta_c}}, \quad (49)$$

$$b_D := a \log \frac{2(1 - A_c)}{A_c' r_c}. \quad (50)$$

The quantity β_c in the above expressions reads

$$\beta_c = \frac{\mathcal{F}_c(1 - A_c)^2}{2C_c A_c^2} [\mathcal{F}_c(C_c'' A_c - C_c A_c'') + (3C_c' A_c + C_c A_c') \mathcal{F}_c' + 2A_c C_c \mathcal{F}_c'']. \quad (51)$$

Note that we use the subscript c to indicate evaluation at r_c . Additionally, we remind the reader that the function $R(z, r_c, E)$ is defined in Eq. (35), while r_c is given by Eq. (30). Now, expressing Eq. (47) as a series in δ and retaining only the leading term gives

$$I(r_0, E) = \int_0^1 g(z, r_c, E) dz + \mathcal{O}(\delta) := b_R. \quad (52)$$

In the strong deflection limit, the deflection angle (33) is then found to be

$$\hat{\alpha}(r_0, E) = -a \log \delta(r_0, E) + b, \quad (53)$$

Above, $\delta(r_0, E) = r_0/r_c(E) - 1 \ll 1$, see Eq. (40), a is defined by Eq. (49) and $b := b_D + b_R - \pi$, with b_D and b_R given by Eqs. (50) and (52), respectively.

Eq. (53) can also be expressed as a function of the impact parameter u . For massive particles, the impact parameter is defined as [18]

$$u^2 = \frac{L^2}{E^2 - 1}. \quad (54)$$

Using Eq. (12), we can express u in terms of the closest approach distance r_0 and the particle's energy E as

$$u^2 = \frac{\mathcal{F}_0^2 C_0}{1 - \frac{1}{E^2} A_0}. \quad (55)$$

In the limit $r_0 \rightarrow r_c$, u converges to u_c , which corresponds to the value for massive particles coming from infinity and entering the circular orbit. Therefore, we introduce a parameter $\varepsilon \ll 1$ through the equation

$$u := u_c(1 + \varepsilon), \quad u_c = \sqrt{\frac{\mathcal{F}_c^2 C_c}{1 - \frac{1}{E^2} A_c}}. \quad (56)$$

Next, by approximating u for small δ , it follows that

$$u - u_c = \ell r_c^2 \delta^2 = u_c \varepsilon, \quad (57)$$

with ℓ given by

$$\ell := \frac{\beta_c A_c'^2 \sqrt{C_c}}{2\mathcal{F}_c A_c^{3/2} (1 - A_c)^2 \sqrt{1 - 1/E^2}}. \quad (58)$$

In the strong deflection limit, as a function of the impact parameter, Eq. (53) results in

$$\hat{\alpha}(u, E) = -\bar{a} \log \varepsilon(u, E) + \bar{b}, \quad (59)$$

with $\varepsilon(u, E) = u/u_c(E) - 1 \ll 1$ and the coefficients \bar{a} and \bar{b} expressed as

$$\bar{a} := \frac{a}{2} = \frac{R(0, r_c, E)}{2\sqrt{\beta_c}}, \quad (60)$$

$$\bar{b} := -\pi + b_R + \bar{a} \log \frac{2\beta_c}{\mathcal{F}_c^2 A_c}, \quad (61)$$

respectively.

As anticipated, in certain applications, it may be more convenient to use the asymptotic velocity at infinity, denoted by v , instead of the energy E . To rewrite all the formulas in terms of velocity rather than energy, we can simply perform the substitution

$$E = \frac{1}{\sqrt{1 - v^2}}. \quad (62)$$

V. APPLICATIONS

The general formulas presented in the previous section, valid for static, asymptotically flat and spherically symmetric spacetimes, can now be specialized to particular cases. After reproducing the already known results for the Schwarzschild metric (see Ref. [84] for further details), we will consider the Reissner-Nordström and Janis-Newman-Winicour metrics.

A. Schwarzschild metric

As already anticipated in Sec. III, in this case the metric coefficients are

$$A(r) = 1 - \frac{1}{r}, \quad B(r) = \left(1 - \frac{1}{r}\right)^{-1}, \quad C(r) = r^2. \quad (63)$$

The two functions $R(z, r_0, E)$ and $f(z, r_0, E)$ defined in Eqs. (35) and (36), respectively, read

$$R(z, r_0, E) = 2\mathcal{F}_0 = 2\sqrt{1 - \left(1 - \frac{1}{r_0}\right) \frac{1}{E^2}}, \quad (64)$$

$$f(z, r_0, E) = \frac{1}{\sqrt{\alpha z + \beta z^2 - \gamma z^3}}, \quad (65)$$

where the coefficients α, β and γ are given by

$$\alpha = \alpha(r_0, E) = 2 - \frac{3}{r_0} - \frac{2}{E^2} \left(1 - \frac{2}{r_0} + \frac{1}{r_0^2}\right), \quad (66)$$

$$\beta = \beta(r_0, E) = \frac{3}{r_0} - 1 + \frac{1}{E^2} \left(1 - \frac{4}{r_0} + \frac{3}{r_0^2}\right), \quad (67)$$

$$\gamma = \gamma(r_0, E) = \frac{1}{r_0} \left[1 - \frac{1}{E^2} \left(1 - \frac{1}{r_0}\right)\right]. \quad (68)$$

As $E \rightarrow \infty$, it is immediate to verify that Eq. (65) reduce to Eq. (42) of Ref. [14]. Now, the radius of the unstable

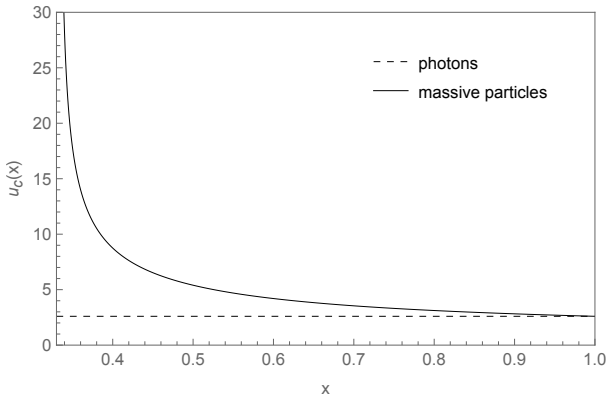


Figure 1. Critical impact parameter for massive particles given by Eq. (78) as a function of the variable $x = x(E)$, which is defined in Eq. (29). In the limit $x \rightarrow 1$ (which corresponds to the limit $E \rightarrow \infty$), the critical impact parameter approaches the corresponding value for photons, i.e., $\lim_{x \rightarrow 1} \bar{u}_c(x) = 3\sqrt{3}/2$ [14]. In the plot, this is represented by the dotted horizontal line. The critical impact parameter for deflection increases for lower-energy particles, diverging for particles at rest at infinity, corresponding to $x = 1/3$.

circular orbit can be found by setting $\alpha(r_0, E) = 0$, resulting in Eq. (30), with $x = x(E)$ defined in Eq. (29). From Eqs. (49), (50) and (52), we then obtain the various coefficients of the strong deflection limit analysis in terms of x , that is

$$a = a(x) = 2\sqrt{\frac{1+x}{2x}}, \quad (69)$$

$$b_D = b_D(x) = a \log 2, \quad (70)$$

$$b_R = b_R(x) = -a \log \left[\frac{(\sqrt{3x-1} + \sqrt{6x})^2}{24x} \right]. \quad (71)$$

In terms of the energy per unit rest mass of the particle, as well as of the distance of closest approach, the deflection angle can then be written as

$$\hat{\alpha}(r_0, E) = -2\sqrt{\frac{1+x}{2x}} \log(z_1(x)\delta(r_0, x)) - \pi, \quad (72)$$

where the quantity z_1 is defined by

$$z_1(x) := \frac{9x - 1 + 2\sqrt{6x(3x-1)}}{48x}, \quad (73)$$

with $x = x(E)$ given by Eq. (29). Eq. (72) agrees with Eq. (53) in Ref. [84].

In terms of the impact parameter u , the deflection angle instead results in

$$\hat{\alpha}(u, E) = -\bar{a}(x) \log \varepsilon(u, x) + \bar{b}(x), \quad (74)$$

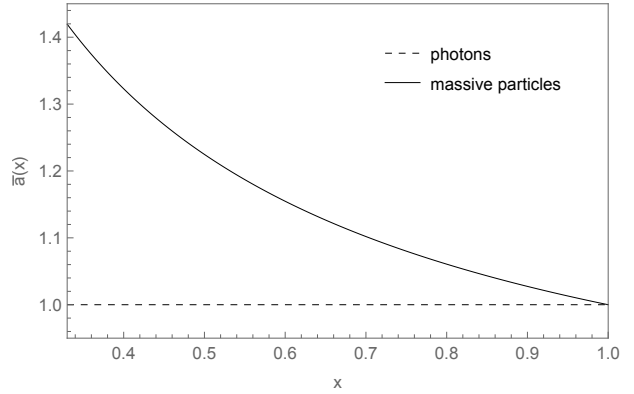


Figure 2. Behavior of the strong deflection limit coefficient $\bar{a}(x)$ defined in Eq. (76) in Sec. V A, which represents the coefficient of the logarithmic divergence. As expected, in the limit $x \rightarrow 1$, $\bar{a}(x)$ approaches the corresponding value for photons, i.e., $\lim_{x \rightarrow 1} \bar{a}(x) = 1$ [14].

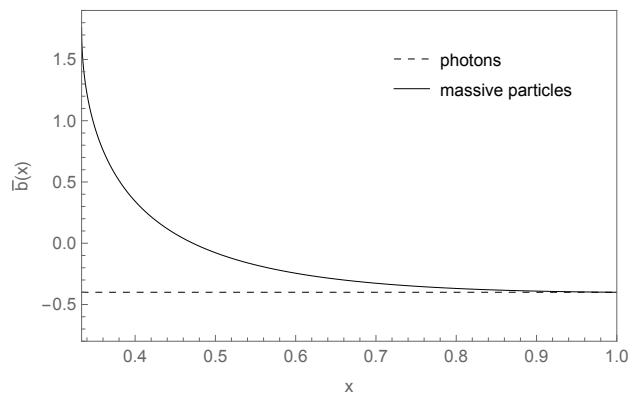


Figure 3. Behavior of the strong deflection limit coefficient $\bar{b}(x)$ defined in Eq. (77), Sec. V A. As expected, in the limit $x \rightarrow 1$, $\bar{b}(x)$ approaches the corresponding value for photons, i.e., $\lim_{x \rightarrow 1} \bar{b}(x) = -0.4002$ [14].

where $\varepsilon(u, x)$, $\bar{a}(x)$ and $\bar{b}(x)$ read

$$\varepsilon(u, x) = \frac{u}{u_c(x)} - 1, \quad (75)$$

$$\bar{a}(x) = \sqrt{\frac{1+x}{2x}}, \quad (76)$$

$$\bar{b}(x) = -\bar{a}(x) \log \left(\frac{2z_1^2(x)}{3x} \right) - \pi, \quad (77)$$

respectively, with $u_c(x)$ given by

$$u_c(x) = \sqrt{\frac{3(1+x)}{3x-1}} r_c(x). \quad (78)$$

Above, $r_c(x)$ is given by Eq. (30). Eq. (74) is in agreement with Eq. (65) in Ref. [84]. The quantities $u_c(x)$, $\bar{a}(x)$ and $\bar{b}(x)$ are plotted in Figs. 1, 2 and 3, respectively. We note that $u_c(x)$ increases as the particle's energy decreases, diverging when the particle originates from rest

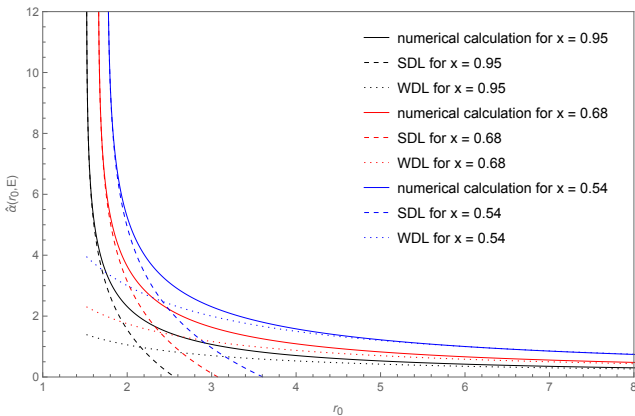


Figure 4. A comparison of the deflection angle for massive particles in a Schwarzschild metric obtained numerically starting from Eq. (17), with that in the weak and strong deflection limits (WDL and SDL, respectively), for different values of x . The deflection angle in a Schwarzschild spacetime in the strong deflection limit is given by Eq. (72), while the formula valid in the weak deflection limit can be found in Ref. [86], Eq. (109). Note that Eq. (17), and Eq. (109) in Ref. [86], are expressed in terms of E and v , respectively. Using Eqs. (29) and (62), we can easily express them in terms of x .

at infinity ($x \rightarrow 1/3$). Both coefficients $\bar{a}(x)$ and $\bar{b}(x)$ also increase at lower energies. Thus, a massive particle experiences stronger deflection than a massless particle coming from infinity with the same impact parameter. In Fig. 4, we present a comparison between the deflection angle obtained numerically and the one obtained analytically in the weak and strong deflection limits, for different values of x . We observe that the deflection angle increases as the energy decreases.

The critical impact parameter for massive particles in

the Schwarzschild metric can also be found in Mielnik and Plebański [72] and Zakharov [81].

B. Reissner-Nordström metric

The Reissner-Nordström metric is a static solution to the Einstein–Maxwell field equations, which describe the gravitational field of a charged, nonrotating and spherically symmetric massive object [117, 118]. In units of $2M$, the metric coefficients in this case are

$$A(r) = B(r)^{-1} = 1 - \frac{1}{r} + \frac{q^2}{r^2}, \quad (79)$$

$$C(r) = r^2, \quad (80)$$

where q denotes the charge parameter of the black hole. The Reissner-Nordström spacetime possesses two concentric horizons located at

$$r_{\pm} = \frac{1}{2} \left(1 \pm \sqrt{1 - 4q^2} \right). \quad (81)$$

As we can deduce from the above equation, these two horizons exist only if $q \in [0, 1/2]$ ($q = 1/2$ corresponds to an extremal black hole), which is thus considered the allowed range for the charge. Therefore, from now on we restrict the charge parameter q to the range $[0, 1/2]$.

We also note that in the Reissner-Nordström case, when finding the inverse function A^{-1} [see Eq. (32)], we obtain a quadratic equation and must choose the outermost branch.

Let us proceed by computing the coefficients α and β , which can easily be found from Eqs. (38) and (39), respectively. The result is

$$\alpha(r_0) = \frac{(q^2 - r_0) \left\{ E^2 r_0^2 [r_0 (2r_0 - 3) + 4q^2] - 2 [r_0 (r_0 - 1) + q^2]^2 \right\}}{r_0^4 E^2 (2q^2 - r_0)}, \quad (82)$$

$$\beta(r_0) = \frac{(q^2 - r_0)^2 [r_0^2 (r_0 - 3) + 9q^2 r_0 - 8q^2] [r_0 (E^2 r_0 - r_0 + 1) - q^2]}{E^2 r_0^4 (2q^2 - r_0)^3}. \quad (83)$$

The above relations reduce to Eqs. (66) and (67) in the limit $q \rightarrow 0$, and to Eqs. (54) and (55) in Ref. [14] in the limit $E \rightarrow \infty$, as expected. In terms of E , the radius of the particle's unstable circular orbit can be found by setting $\alpha(r_0) = 0$, resulting in a quartic equation. In the following, we will consider a perturbative approach. Specifically, we will calculate the coefficients a , b_D and b_R up to order q^2 . Extending the analysis to include higher-order terms is straightforward. For the sake of simplicity, even though perturbative results will be obtained, we will continue using equalities in our equations. The procedure

we follow in order to obtain the quadratic correction to the radius of the unstable circular orbit of the massive particle, r_c , is the same as the one outlined in Sec. V of Ref. [119] for light rays propagating in a plasma environment. In terms of the variable $x = x(E)$, the result one obtains is

$$r_c = r_c(x, q) = 3 \frac{1+x}{1+3x} - \left(1 + \frac{1}{3x} \right) q^2. \quad (84)$$

We can now easily compute the strong deflection limit

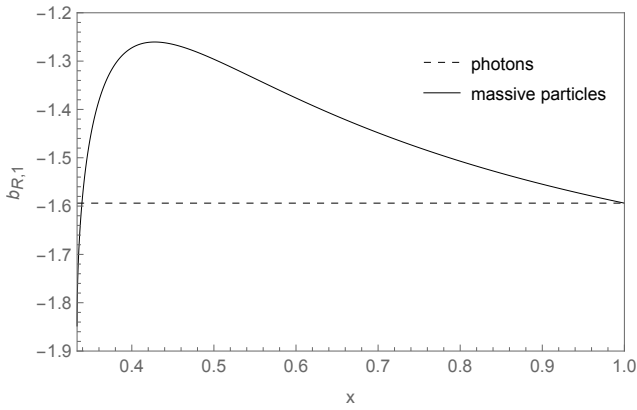


Figure 5. Coefficient $b_{R,1}$ in Eq. (87) in Sec. V B.

coefficients $a = a(x, q)$, $b_D = b_D(x, q)$ and $b_R = b_R(x, q)$. As for the first two coefficients, from Eqs. (49) and (50), we obtain

$$a = \frac{36x^2(x+1) + [3x^2(6x+5) - 1]q^2}{18\sqrt{2x^5(x+1)}}, \quad (85)$$

$$b_D = \frac{1}{18\sqrt{2x^5(x+1)}} \{36x^2(x+1)\log 2 + \{3x^2[6x(2+\log 2) + 4 + \log 32] - \log 2\}q^2\}, \quad (86)$$

respectively.

$$b_{R,1}(z, x) := \frac{(1+3x)^{3/2}}{36x^2} \left(\frac{\sqrt{2}[1-3x(1+2x)]}{z\sqrt{x(1+x)(1+3x)}} + \frac{4\sqrt{3}x(1+x)(1+3x)z^2 \{3x[6x(z^2-3z+1) + z(2z-1) + 3] + z-3\}}{\{(1+x)(1+3x)[3x(2-z) + z]z^2\}^{3/2}} \right). \quad (91)$$

The result of the integral in Eq. (87) is shown in Fig. 5. As we can observe, for small values of x (i.e., for small E), the quadratic correction deviates significantly from the corresponding value calculated for photons [14].

The deflection angle can then be written as a function of r_0 , as well as of x and q , as

$$\hat{\alpha}(r_0, E, q) = -a(x, q) \log \delta(r_0, x, q) + b_D(x, q) + b_R(x, q) - \pi, \quad (92)$$

where $a(x, q)$, $b_D(x, q)$ and $b_R(x, q)$ are given by Eqs. (85), (86) and (87), respectively. We also recall that the quan-

As for the quantity b_R , we recall that it is defined in terms of an integral. The integration can be performed by expanding the integrand (i.e., $g(z, r_c, E)$, see Eq. (44) in Sec. IV for the definition of this function) in powers of q and then evaluating the single coefficients [14]. Up to order q^2 , we get

$$b_R = b_R(x, q) = \int_0^1 g(z, r_c, E) dz = b_{R,0}(x) + b_{R,1}(x)q^2, \quad (87)$$

where $b_{R,0}(x)$ is expressed as

$$b_{R,0}(x) = -a(x, 0) \log \left[\frac{(\sqrt{3x-1} + \sqrt{6x})^2}{24x} \right], \quad (88)$$

$$a(x, 0) = 2\sqrt{\frac{1+x}{2x}}, \quad (89)$$

i.e., the result for an uncharged black hole (Eqs. (88) and (89) indeed coincide with Eqs. (71) and (69), respectively), while the coefficient $b_{R,1}(x)$ is defined as

$$b_{R,1}(x) := \int_0^1 b_{R,1}(z, x) dz, \quad (90)$$

where, in turn, $b_{R,1}(z, x)$ reads

tity $\delta(r_0, x, q)$ is defined by Eq. (40). The formula we derived for the deflection angle, namely Eq. (92), is valid up to order q^2 .

In terms of the impact parameter u , using Eqs. (60) and (61), we obtain

$$\hat{\alpha}(u, E, q) = -\bar{a}(x, q) \log \varepsilon(u, x, q) + \bar{b}(x, q), \quad (93)$$

where the coefficient $\bar{a}(x, q)$ is simply given by $a(x, q)/2$, with $a(x, q)$ expressed by Eq. (49), while $\bar{b}(x, q)$ is calculated from Eq. (61), resulting in

$$\bar{b}(x, q) = -\pi + b_R(x, q) + \frac{2q^2(27x^3 + 3x^2 + x + 1) + \{q^2[3x^2(6x+5) - 1] + 36x^2(x+1)\} \log(6x)}{36\sqrt{2x^5(x+1)}}. \quad (94)$$

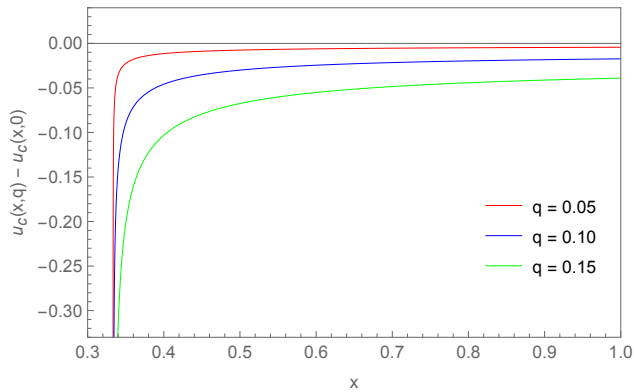


Figure 6. Difference $u_c(x, q) - u_c(x, 0)$ as a function of the particle's energy at infinity, for different values of the charge parameter q . The critical impact parameter $u_c(x, q)$ is defined in Eq. (96), Sec. V B.

In the expression for the deflection angle, Eq. (93), the quantity $\varepsilon(u, x, q)$ reads

$$\varepsilon(u, x, q) = \frac{u}{u_c(x, q)} - 1, \quad (95)$$

where the critical impact parameter $u_c(x, q)$ is obtained from Eq. (55) evaluated at $r = r_c$, giving

$$u_c(x, q) = \frac{3 - q^2 - 3x(q^2 - 1)}{1 + 3x} \sqrt{1 + \frac{4}{3x - 1}}. \quad (96)$$

The critical impact parameter for massive particles in the Reissner-Nordström metric was also carefully investigated in Ref. [81].

As anticipated in Sec. I, the deflection of massive particles was also studied in Ref. [89], where an expression in terms of elliptic integrals was derived. The authors considered various limits but did not derive an expansion in the strong deflection limit comparable to ours. Their Eq. (50) was obtained by expanding the deflection angle around the Schwarzschild photon sphere radius rather than the Reissner-Nordström one. Such an expansion cannot describe the higher-order images in the Reissner-Nordström case, as it does not converge in the strong deflection regime. Moreover, in their treatment, they considered an exact solution for the unstable circular orbit radius, whereas we retained only the quadratic correction in the charge.

We conclude by showing, in Figs. 6, 7 and 8, the quantities $u_c(x, 0) - u_c(x, q)$, $\bar{a}(x, 0) - \bar{a}(x, q)$ and $\bar{b}(x, 0) - \bar{b}(x, q)$, respectively, as functions of x for different values of q . The differences between the various curves vary with the energy. Moreover, for a fixed q , $u_c(x, q)$ decreases as q increases (a consequence of the fact that the horizon shrinks), while $\bar{a}(x, q)$ and $\bar{b}(x, q)$ increases as q increases.

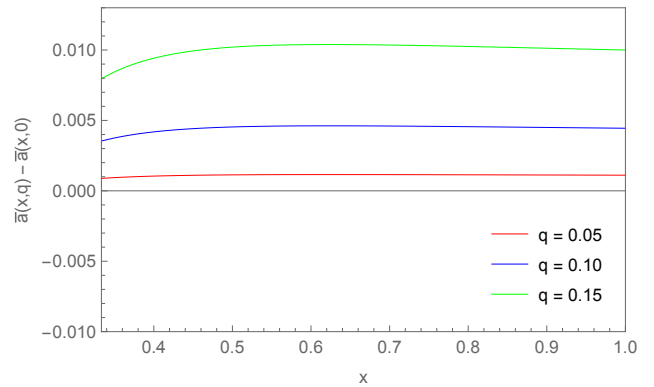


Figure 7. Difference $\bar{a}(x, q) - \bar{a}(x, 0)$ as a function of the particle's energy, for different values of the charge parameter q . The strong deflection limit coefficient $\bar{a}(x, q)$ is defined by $a(x, q)/2$, with $a(x, q)$ given by Eq. (85) (Sec. V B).

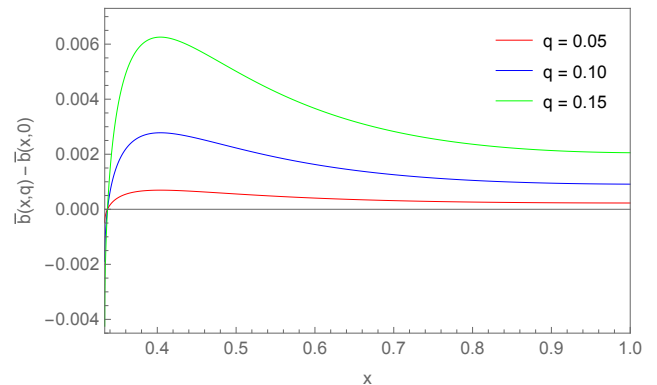


Figure 8. Difference $\bar{b}(x, q) - \bar{b}(x, 0)$ as a function of the particle's energy, for different values of charge parameter q . The strong deflection limit coefficient $\bar{b}(x, q)$ is given by Eq. (94) in Sec. V B.

C. Janis-Newman-Winicour metric

Here, we consider the Janis-Newman-Winicour metric, which is the unique static and spherically symmetric solution to the Einstein equations for a massless, minimally coupled scalar field [120–123]. This solution is characterized by the mass M and a parameter γ related to the scalar field strength. Taking $r_\gamma = 2M/\gamma$ as the unit of measure of distances, the metric coefficients are [68]

$$A(r) = \left(1 - \frac{1}{r}\right)^\gamma, \quad (97)$$

$$B(r) = \left(1 - \frac{1}{r}\right)^{-\gamma}, \quad (98)$$

$$C(r) = \left(1 - \frac{1}{r}\right)^{1-\gamma} r^2, \quad (99)$$

with the scalar field given by

$$\Phi(r) = \sqrt{\frac{1 - \gamma^2}{16\pi}} \log\left(1 - \frac{1}{r}\right). \quad (100)$$

The dimensionless parameter γ appearing in the above relations takes values in the range $0 < \gamma \leq 1$. However, as we shall see, the perturbative character of the analysis below significantly narrows down the admissible range of γ . As one can easily check, when $\gamma = 1$, the Schwarzschild solution is recovered. Moreover, as shown in Ref. [124], the Janis-Newman-Winicour solution has

a naked curvature singularity located at $r = r_\gamma$. When γ is relatively close to unity, the spacetime under investigation admits the existence of unstable circular orbits which are always external to r_γ [125].

As already anticipated, we proceed by working in a perturbative scheme. The coefficients α and β , as well as the expansion of r_c up to order $(\gamma - 1)$, result to be

$$\alpha(r_0) = \frac{r_0^{-2\gamma} [r_0^\gamma - (r_0 - 1)^\gamma] [E^2 r_0^\gamma (2r_0 - 2\gamma - 1) + (\gamma - 2r_0 + 1)(r_0 - 1)^\gamma]}{\gamma E^2}, \quad (101)$$

$$\beta(r_0) = \frac{\left[\left(\frac{r_0 - 1}{r_0} \right)^\gamma - 1 \right]^2 \left[\left(\frac{r_0 - 1}{r_0} \right)^\gamma - E^2 \right] r_0^\gamma (r_0 - 1)^{-\gamma} \{ 3\gamma + 1 + 2 [\gamma^2 - 3\gamma r_0 + r_0(r_0 - 1)] \}}{2\gamma^2 E^2}, \quad (102)$$

$$r_c(x, \gamma) = 1 + \frac{2}{3x + 1} + \frac{(\gamma - 1)(1 + x) \left[9x^2 + 6x \left(3 + \log \frac{9}{4} \right) + 12(x - 1) \log(1 + x) + 5 - 12 \log \frac{3}{2} \right]}{4x(1 + 3x)^2}. \quad (103)$$

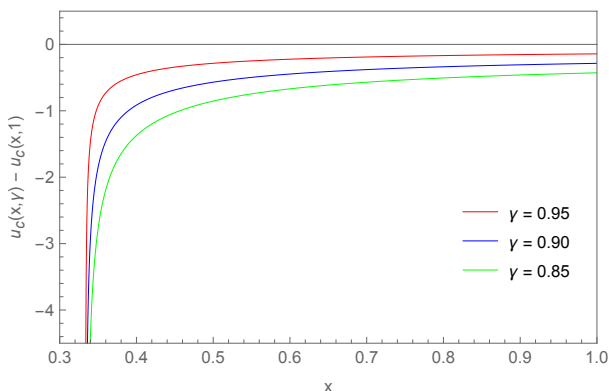


Figure 9. Difference $u_c(x, \gamma) - u_c(x, 1)$ as a function of x , for different values of the parameter γ . The quantity $u_c(x, \gamma)$ is defined in Eq. (96) (Sec. V C).

The above relations reduce to Eqs. (66), (67) and (30) in the limit $q \rightarrow 0$, and to Eqs. (54) and (55) in Ref. [14] in the limit $E \rightarrow \infty$, as expected. From Eqs. (101), (102) and (103), the strong deflection limit coefficients can be easily calculated, proceeding in exactly the same way as we did in the previous two sections. The deflection angle is then obtained as

$$\hat{\alpha}(r_0, E, \gamma) = -a(x, \gamma) \log \delta(r_0, x, \gamma) + b_D(x, \gamma) + b_R(x, \gamma) - \pi, \quad (104)$$

where the coefficients $a(x, \gamma)$, $b_D(x, \gamma)$ and $b_R(x, \gamma)$ are given by Eqs. (A1), (A2) and (A3)–(A4) in the Appendix, respectively. We remind the reader that the quantity $x = x(E)$ is defined in Eq. (29).

In terms of the impact parameter, the deflection angle instead results in

$$\hat{\alpha}(u, E, \gamma) = -\bar{a}(x, \gamma) \log \varepsilon(u, x, \gamma) + \bar{b}(x, \gamma), \quad (105)$$

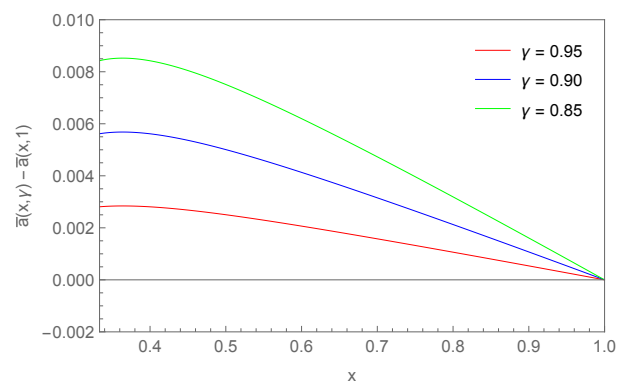


Figure 10. Difference $\bar{a}(x, \gamma) - \bar{a}(x, 1)$ as a function of the particle's energy, for different values of the parameter γ . The coefficient $\bar{a}(x, \gamma)$ is defined by $\bar{a}(x, \gamma) = a(x, \gamma)/2$, with $a(x, \gamma)$ given by Eq. (A1) (Sec. V C).

where $\bar{a}(x, \gamma) = a(x, \gamma)/2$, with $a(x, \gamma)$ given by Eq. (A1), $\bar{b}(x, \gamma)$ given by Eq. (A5), and $\varepsilon(u, x, \gamma)$ expressed as

$$\varepsilon(u, x, \gamma) = \frac{u}{u_c(x, \gamma)} - 1, \quad (106)$$

$$u_c(x, \gamma) = \frac{3}{2} \sqrt{\frac{3}{9x^2 - 1}} \left[\frac{2(1+x)^{\frac{3}{2}}}{\sqrt{1+3x}} + (3x+5) \times \left(\frac{1+x}{1+3x} \right)^{\frac{3}{2}} \log \frac{3(1+x)}{2} (\gamma - 1) \right]. \quad (107)$$

The differences $u_c(x, \gamma) - u_c(x, 0)$, $\bar{a}(x, \gamma) - \bar{a}(x, 0)$ and $\bar{b}(x, \gamma) - \bar{b}(x, 0)$ as functions of x , fixed γ , are plotted in Figs. 9, 10 and 11, respectively. Comparing with Figs. 6, 7 and 8, we observe that the phenomenology arising from the Janis-Newman-Winicour spacetime differs fundamentally from that of the Reissner-Nordström spacetime, allowing for potential distinction. In Fig. 9, we

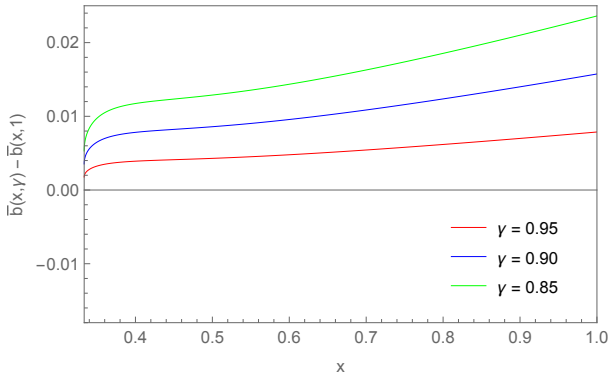


Figure 11. Difference $\bar{b}(x, \gamma) - \bar{b}(x, 1)$ as a function of x , for different values of the parameter γ . The coefficient $\bar{b}(x, \gamma)$ is given by Eq. (A5) (Sec. V C).

observe that the coefficient $\bar{a}(x, \gamma)$ approaches unity as $x \rightarrow 1$, in agreement with the findings in Ref. [14].

We note that, as γ decreases, $u_c(x, \gamma)$ decreases, while the deflection coefficients \bar{a} and \bar{b} increase, similar to the Reissner-Nordström case. However, significant differences arise at different energies; in Fig. 7, we show that in Reissner-Nordström case, the increase in \bar{a} with charge affects all energies, whereas in Janis-Newman-Winicour case, this increase is much more pronounced at lower energies. This indicates that deflection of massive particles can help distinguish metrics that appear degenerate when studied using massless particles alone. We remind that the variable x , see Eq. (29), is a monotonic function of E : small values of E correspond to small values of x , and large values of E correspond to large values of x .

VI. DISCUSSION AND CONCLUSIONS

This study extends the understanding of gravitational deflection of massive particles by very compact objects. By employing the strong deflection limit approximation, the research delves into the behavior of massive parti-

cles traveling along timelike geodesics, particularly when these particles approach a compact object at a radius close to that of the unstable circular orbit. This scenario, where particles circle the object before eventually escaping, mirrors the lensing effects observed for light, thereby extending the application of gravitational lensing principles to particles with mass.

The key contribution of this work is the development of a general solution for the deflection angle of massive particles in the strong deflection limit. Unlike previous studies that focused on specific spacetime metrics, this study provides a framework applicable to any static, asymptotically flat and spherically symmetric spacetime, making it relevant to a wider range of astrophysical scenarios.

In terms of the closest approach distance, the formula for the deflection angle is given by Eq. (53), while as a function of the impact parameter it is given by Eq. (59). Recall that, unlike light rays, the deflection of massive particles depends on two parameters rather than one. Here, we choose the particle's energy at infinity per unit rest mass, E , as one of these parameters. Note that in most formulas, the energy appears only within the quantity $x = x(E)$, defined in Eq. (29). Alternatively, one can use the velocity at infinity by applying substitution (62).

As an application, the formulas of Sec. IV have been specialized to the Schwarzschild, Reissner-Nordström and Janis-Newman-Winicour metrics. In terms of r_0 , the deflection angle is given by Eq. (72) for Schwarzschild, Eq. (92) for Reissner-Nordström and Eq. (104) for Janis-Newman-Winicour. Alternatively, in terms of u , it is given by Eq. (74) for Schwarzschild, Eq. (93) for Reissner-Nordström and Eq. (105) for Janis-Newman-Winicour.

ACKNOWLEDGEMENTS

OYT acknowledges support from the ERC Advanced Grant “JETSET: Launching, propagation and emission of relativistic jets from binary mergers and across mass scales” (Grant No. 884631). OYT also thanks Valerio Bozza and his group for their hospitality during a visit to the University of Salerno.

Appendix A: Strong deflection limit coefficients for massive particles in Janis-Newman-Winicour spacetime

In this Appendix, we report the analytical expressions for the strong deflection limit coefficients in the case of the Janis-Newman-Winicour metric, see Sec. V C.

The coefficients $a(x, \gamma)$ and $b_D(x, \gamma)$ are obtained as

$$a(x, \gamma) = \frac{\sqrt{1+x} \left\{ 48x^2 + (\gamma - 1)(x - 1) \left[3x(3x - 4) + 12 \log \frac{3(x+1)}{2} - 5 \right] \right\}}{24\sqrt{2}x^{5/2}}, \quad (\text{A1})$$

$$b_D(x, \gamma) = \sqrt{\frac{2(1+x)}{x}} \left\{ \log 2 + (\gamma - 1) \left[\frac{(x-1) \log 2}{48x^2} \left(9x^2 - 12x - 5 + 12 \log \frac{3(1+x)}{2} \right) - \frac{3x - 3(1+x) \log \frac{3(1+x)}{2} + 1}{3x + 1} \right] \right\}. \quad (\text{A2})$$

The coefficient $b_R(x, \gamma)$ is given by

$$b_R(x, \gamma) = -2\sqrt{\frac{1+x}{2x}} \log \left[\frac{(\sqrt{3x-1} + \sqrt{6x})^2}{24x} \right] + (\gamma - 1) \int_0^1 b_{R,1}(z, x) dz, \quad (\text{A3})$$

where, in turn, the integrand $b_{R,1}(z, x)$ is expressed as

$$\begin{aligned} b_{R,1}(z, x) = & \frac{(1-x^2) \left[3x(3x-4) + 12 \log \frac{3(1+x)}{2} - 5 \right]}{24\sqrt{2x^5(1+x)}z} + \{z[3x(2-z) - z][12x(2-z)(z-1) + z(6-5z)] \\ & + 9x^2z(z-2)\} \left[5 + 9x^2 + 6x \left(3 + \log \frac{9}{4} \right) - 12 \log \frac{3}{2} + 12(x-1) \log(1+x) \right] \\ & + 3z^2[3x(z-2) + z]^2 \left\{ x \left[9x^2 - 3x(13 + \log 16) - 29 + 8 \log \frac{6561}{32} \right] + 64x \log(1+x) \right. \\ & + 12(x-1)^2 \log 3(x+1) - 5 - 12 \log 2 \} + 24x[3x(2-z) - z] \left\{ [6x(z-1)(5z^2 - 6z - 1) \right. \\ & \left. + 10 + 9x^2z - 15z + 2z^2(5z-3)] \log \frac{3(1+x)}{2} + (z-1)(z+3xz+2)[z+3x(1+z)+5] \right\} \\ & \times [(1+x)(1+3x)] \left\{ 8\sqrt{3x}[3x(z-2) + z]^2 [z(1+3x)]^2 \sqrt{z^2(1+x)[3x(2-z) - z]} \right\}^{-1}. \quad (\text{A4}) \end{aligned}$$

Finally, the expression for the coefficient $\bar{b}(x, \gamma)$ is

$$\begin{aligned} \bar{b}(x, \gamma) = & -\pi + b_R(x, \gamma) + \frac{\sqrt{1+x}}{2x} \left\{ \log 6 + \frac{\gamma-1}{1+3x} \left\{ [24x(9x^2 + 11x + 3) - 12] \log \frac{3(1+x)}{2} \right. \right. \\ & \left. \left. - 2 \{ 5 + 9x[3 + x(6x^2 + 17x + 9)] \} + (x-1) \log 6 \{ (3x-5)(1+3x)^2 \right. \right. \\ & \left. \left. + 12[(1+6x) \log 3(1+x) - 3x \log 6(1+x) - \log 2] \} \right\} \right\}. \quad (\text{A5}) \end{aligned}$$

-
- [1] Event Horizon Telescope Collaboration, K. Akiyama, A. Alberdi, W. Alef, K. Asada, R. Azulay, A.-K. Baczko, D. Ball, et al., First M87 Event Horizon Telescope results. I. The shadow of the supermassive black hole, *The Astrophysical Journal Letters* **875**, L1 (2019).
- [2] Event Horizon Telescope Collaboration, K. Akiyama, A. Alberdi, W. Alef, K. Asada, R. Azulay, A.-K. Baczko, D. Ball, et al., First M87 Event Horizon Telescope results. II. Array and instrumentation, *The Astrophysical Journal Letters* **875**, L2 (2019).
- [3] Event Horizon Telescope Collaboration, K. Akiyama, A. Alberdi, W. Alef, K. Asada, R. Azulay, A.-K. Baczko, D. Ball, et al., First M87 Event Horizon Telescope results. III. Data processing and calibration, *The Astrophysical Journal Letters* **875**, L3 (2019).
- [4] Event Horizon Telescope Collaboration, K. Akiyama, A. Alberdi, W. Alef, K. Asada, R. Azulay, A.-K. Baczko, D. Ball, et al., First M87 Event Horizon Telescope results. IV. Imaging the central supermassive black hole, *The Astrophysical Journal Letters* **875**, L4 (2019).
- [5] Event Horizon Telescope Collaboration, K. Akiyama, A. Alberdi, W. Alef, K. Asada, R. Azulay, A.-K. Baczko, D. Ball, et al., First M87 Event Horizon Telescope results. V. Physical origin of the asymmetric ring, *The Astrophysical Journal Letters* **875**, L5 (2019).
- [6] Event Horizon Telescope Collaboration, K. Akiyama, A. Alberdi, W. Alef, K. Asada, R. Azulay, A.-K. Baczko, D. Ball, et al., First M87 Event Horizon Telescope results. VI. The shadow and mass of the central black hole, *The Astrophysical Journal Letters* **875**, L6 (2019).
- [7] Event Horizon Telescope Collaboration, Event Horizon Telescope Collaboration, K. Akiyama, A. Alberdi, W. Alef, J. C. Algaba, R. Anantua, K. Asada, R. Azulay, et al., First Sagittarius A* Event Horizon Telescope results. I. The shadow of the supermassive black hole in the center of the Milky Way, *The Astrophysical Journal Letters* **930**, L12 (2022).
- [8] Event Horizon Telescope Collaboration, K. Akiyama, A. Alberdi, W. Alef, J. C. Algaba, R. Anantua, K. Asada, R. Azulay, et al., First Sagittarius A* Event Horizon Telescope results. II. EHT and multiwavelength observations, data processing, and calibration, *The Astrophysical Journal Letters* **930**, L13 (2022).
- [9] Event Horizon Telescope Collaboration, K. Akiyama, A. Alberdi, W. Alef, J. C. Algaba, R. Anantua, K. Asada, R. Azulay, et al., First Sagittarius A* Event Horizon Telescope results. III. Imaging of the Galactic center supermassive black hole, *The Astrophysical Journal Letters* **930**, L14 (2022).
- [10] Event Horizon Telescope Collaboration, K. Akiyama, A. Alberdi, W. Alef, J. C. Algaba, R. Anantua, K. Asada, R. Azulay, et al., First Sagittarius A* Event Horizon

- Telescope results. IV. Variability, morphology, and black hole mass, *The Astrophysical Journal Letters* **930**, L15 (2022).
- [11] Event Horizon Telescope Collaboration, K. Akiyama, A. Alberdi, W. Alef, J. C. Algaba, R. Anantua, K. Asada, R. Azulay, et al., First Sagittarius A* Event Horizon Telescope results. V. Testing astrophysical models of the Galactic center black hole, *The Astrophysical Journal Letters* **930**, L16 (2022).
- [12] Event Horizon Telescope Collaboration, K. Akiyama, A. Alberdi, W. Alef, J. C. Algaba, R. Anantua, K. Asada, R. Azulay, et al., First Sagittarius A* Event Horizon Telescope results. VI. Testing the black hole metric, *The Astrophysical Journal Letters* **930**, L17 (2022).
- [13] C. Darwin, The gravity field of a particle, *Proceedings of the Royal Society of London, Series A, Mathematical and Physical Sciences* **249**, 180 (1959).
- [14] V. Bozza, Gravitational lensing in the strong field limit, *Physical Review D* **66**, 103001 (2002).
- [15] V. Bozza, Quasiequatorial gravitational lensing by spinning black holes in the strong field limit, *Physical Review D* **67**, 103006 (2003).
- [16] D. Hilbert, Die Grundlagen der Physik (Zweite Mitteilung), *Nachr. Gesellsch. Wissensch. Göttingen, Math.-Phys. Kl.* **1917**, 53 (1917).
- [17] R. d'E. Atkinson, On light tracks near a very massive star, *Astronomical Journal* **70**, 517 (1965).
- [18] C. W. Misner, K. S. Thorne, and J. A. Wheeler, *Gravitation* (W. H. Freeman, San Francisco, 1973).
- [19] J.-P. Luminet, Image of a spherical black hole with thin accretion disk, *Astronomy and Astrophysics* **75**, 228–235 (1979).
- [20] H. C. Ohanian, The black hole as a gravitational “lens”, *American Journal of Physics* **55**, 428–432 (1987).
- [21] K. S. Virbhadra and G. F. R. Ellis, Schwarzschild black hole lensing, *Physical Review D* **62**, 084003 (2000).
- [22] S. Frittelli, T. P. Kling, and E. T. Newman, Spacetime perspective of Schwarzschild lensing, *Physical Review D* **61**, 064021 (2000).
- [23] C.-M. Claudel, K. S. Virbhadra, and G. F. R. Ellis, The geometry of photon surfaces, *Journal of Mathematical Physics* **42**, 818–838 (2001).
- [24] V. Bozza, S. Capozziello, G. Iovane, and G. Scarpetta, Strong field limit of black hole gravitational lensing, *General Relativity and Gravitation* **33**, 1535–1548 (2001).
- [25] W. Hasse and V. Perlick, Gravitational lensing in spherically symmetric static spacetimes with centrifugal force reversal, *General Relativity and Gravitation* **34**, 415–433 (2002).
- [26] A. M. Beloborodov, Gravitational bending of light near compact objects, *The Astrophysical Journal* **566**, L85 (2002).
- [27] V. Perlick, Gravitational lensing from a spacetime perspective, *Living Reviews in Relativity* **7**, 9 (2004).
- [28] V. Perlick, Exact gravitational lens equation in spherically symmetric and static spacetimes, *Physical Review D* **69**, 064017 (2004).
- [29] P. Amore and S. Arceo, Analytical formulas for gravitational lensing, *Physical Review D* **73**, 083004 (2006).
- [30] P. Amore, M. Cervantes, A. De Pace, and F. M. Fernández, Gravitational lensing from compact bodies: Analytical results for strong and weak deflection limits, *Physical Review D* **75**, 083005 (2007).
- [31] S. V. Iyer and A. O. Petters, Light’s bending angle due to black holes: from the photon sphere to infinity, *General Relativity and Gravitation* **39**, 1563–1582 (2007).
- [32] E. Hackmann and C. Lämmerzahl, Complete analytic solution of the geodesic equation in Schwarzschild – (anti-)de Sitter spacetimes, *Physical Review Letters* **100**, 171101 (2008).
- [33] E. Hackmann and C. Lämmerzahl, Geodesic equation in Schwarzschild – (anti-)de Sitter space-times: Analytical solutions and applications, *Physical Review D* **78**, 024035 (2008).
- [34] K. S. Virbhadra and C. R. Keeton, Time delay and magnification centroid due to gravitational lensing by black holes and naked singularities, *Physical Review D* **77**, 124014 (2008).
- [35] G. S. Bisnovatyi-Kogan and O. Yu. Tsupko, Strong gravitational lensing by Schwarzschild black holes, *Astrophysics* **51**, 99–111 (2008).
- [36] N. Mukherjee and A. S. Majumdar, Rotating brane-world black hole lensing in the strong deflection limit, *Gravitation and Cosmology* **15**, 263–272 (2009).
- [37] V. Bozza, Gravitational lensing by black holes, *General Relativity and Gravitation* **42**, 2269–2300 (2010).
- [38] A. Tarasenko, Reconstruction of a compact object motion in the vicinity of a black hole by its electromagnetic radiation, *Physical Review D* **81**, 123005 (2010).
- [39] E. F. Eiroa and C. M. Sendra, Gravitational lensing by a regular black hole, *Classical and Quantum Gravity* **28**, 085008 (2011).
- [40] S.-W. Wei, Yu.-X. Liu, C.-E. Fu, and K. Yang, Strong field limit analysis of gravitational lensing in Kerr-Taub-NUT spacetime, *Journal of Cosmology and Astroparticle Physics*, 10 (2012) 053.
- [41] G. Li, Y. Zhang, L. Zhang, Z. Feng, and X. Zu, Strong gravitational lensing in the Einstein-Proca theory, *International Journal of Theoretical Physics* **54**, 1245–1252 (2015).
- [42] O. Semerák, Approximating light rays in the Schwarzschild field, *The Astrophysical Journal* **800**, 77 (2015).
- [43] A. Alhamzawi and R. Alhamzawi, Gravitational lensing in the strong field limit by modified gravity, *General Relativity and Gravitation* **48**, 167 (2016).
- [44] N. Tsukamoto, Strong deflection limit analysis and gravitational lensing of an Ellis wormhole, *Physical Review D* **94**, 124001 (2016).
- [45] G. F. Aldi and V. Bozza, Relativistic iron lines in accretion disks: The contribution of higher order images in the strong deflection limit, *Journal of Cosmology and Astroparticle Physics* 02 (2017) 033.
- [46] D.-C. Dai, D. Stojkovic, and G. D. Starkman, Strong lensing constraints on modified gravity models, *Physical Review D* **98**, 124027 (2018).
- [47] F. Aratore and V. Bozza, Decoding a black hole metric from the interferometric pattern of the relativistic images of a compact source, *Journal of Cosmology and Astroparticle Physics* 10 (2021) 054.
- [48] X.-M. Kuang, Z.-Y. Tang, B. Wang, and A. Wang, Constraining a modified gravity theory in strong gravitational lensing and black hole shadow observations, *Physical Review D* **106**, 064012 (2022).
- [49] A. Cieřlik and P. Mach, Revisiting timelike and null geodesics in the Schwarzschild spacetime: general expressions in terms of Weierstrass elliptic functions, *Classical and Quantum Gravity* **39**, 225003 (2022).

- [50] A. Cieřlik, E. Hackmann, and P. Mach, Kerr geodesics in terms of Weierstrass elliptic functions, *Physical Review D* **108**, 024056 (2023).
- [51] F. Aratore and V. Bozza, Analytical perturbations of relativistic images in Kerr space-time, *Journal of Cosmology and Astroparticle Physics* **07** (2024) 033.
- [52] J. Claros and E. Gallo, Accurate analytical modeling of light rays in spherically symmetric spacetimes: Applications in the study of black hole accretion disks and polarimetry, *Physical Review D* **109**, 124055 (2024).
- [53] S. E. Gralla, D. E. Holz, and R. M. Wald, Black hole shadows, photon rings, and lensing rings, *Physical Review D* **100**, 024018 (2019).
- [54] M. D. Johnson, A. Lupsasca, A. Strominger, G. N. Wong, S. Hadar, D. Kapec, R. Narayan, A. Chael, C. F. Gammie, P. Galison, et al., Universal interferometric signatures of a black hole’s photon ring, *Science Advances* **6**, eaaz1310 (2020).
- [55] S. E. Gralla and A. Lupsasca, Observable shape of black hole photon rings, *Physical Review D* **102**, 124003 (2020).
- [56] S. E. Gralla, A. Lupsasca, D. P. Marrone, The shape of the black hole photon ring: A precise test of strong-field general relativity, *Physical Review D* **102**, 124004 (2020).
- [57] S. E. Gralla and A. Lupsasca, Lensing by Kerr black holes, *Physical Review D* **101**, 044031 (2020).
- [58] M. Wielgus, Photon rings of spherically symmetric black holes and robust tests of non-Kerr metrics, *Physical Review D* **104**, 124058 (2021).
- [59] A. E. Broderick, P. Tiede, D. W. Pesce, and R. Gold, Measuring spin from relative photon ring sizes, *The Astrophysical Journal* **927**, 6 (2022).
- [60] D. Ayzenberg, Testing gravity with black hole shadow subrings, *Classical and Quantum Gravity* **39**, 105009 (2022).
- [61] M. Guerrero, G. J. Olmo, D. Rubiera-Garcia, and D. S.-C. Gómez, Multiring images of thin accretion disk of a regular naked compact object, *Physical Review D* **106**, 044070 (2022).
- [62] G. S. Bisnovatyi-Kogan and O. Yu Tsupko, Analytical study of higher-order ring images of the accretion disk around a black hole, *Physical Review D* **105**, 064040 (2022).
- [63] O. Yu Tsupko, Shape of higher-order images of equatorial emission rings around a Schwarzschild black hole: Analytical description with polar curves, *Physical Review D* **106**, 064033 (2022).
- [64] A. Eichhorn, A. Held, and P.-V. Johannsen, Universal signatures of singularity-resolving physics in photon rings of black holes and horizonless objects, *Journal of Cosmology and Astroparticle Physics* **01** (2023) 043.
- [65] A. E. Broderick, K. Salehi, and B. Georgiev, Shadow implications: What does measuring the photon ring imply for gravity?, *The Astrophysical Journal* **958**, 114 (2023).
- [66] P. Kocherlakota, L. Rezzolla, R. Roy, and M. Wielgus, Prospects for future experimental tests of gravity with black hole imaging: Spherical symmetry, *Physical Review D* **109**, 064064 (2024).
- [67] P. Kocherlakota, L. Rezzolla, R. Roy, and M. Wielgus, Hotspots and photon rings in spherically symmetric space-times, *Monthly Notices of the Royal Astronomical Society* **531**, 3606 (2024).
- [68] F. Aratore, O. Yu. Tsupko, and V. Perlick, Constraining spherically symmetric metrics by the gap between photon rings, *Physical Review D* **109**, 124057 (2024).
- [69] Y. Hagihara, Theory of the relativistic trajectories in a gravitational field of Schwarzschild, *Japanese Journal of Astronomy and Geophysics* **8**, 67 (1931).
- [70] C. Darwin, The gravity field of a particle. II, *Proceedings of the Royal Society of London, Series A, Mathematical and Physical Sciences* **263**, 39 (1961).
- [71] A. F. Bogorodsky, Einstein’s field equations and their application to astronomy (in Russian), Kiev University, Kiev (1962).
- [72] B. Mielnik and J. Plebański, A study of geodesic motion in the field of Schwarzschild’s solution, *Acta Physica Polonica* **21**, 239 (1962).
- [73] A. W. K. Metzner, Observable properties of large relativistic masses, *Journal of Mathematical Physics* **4**(9), 1194 (1963).
- [74] Ya. B. Zel’dovich and I. D. Novikov, *The theory of gravitation and stellar evolution* (Nauka, Moscow, 1971).
- [75] S. Weinberg, *Gravitation and cosmology: principles and applications of the general theory of relativity* (John Wiley and Sons, New York, 1972).
- [76] M. P. Silverman, Gravitational deflection of relativistic massive particles, *American Journal of Physics* **48**, 72 (1980).
- [77] S. Chandrasekhar, *The mathematical theory of black holes* (Oxford University Press, Oxford, England, 1983).
- [78] C. Miró Rodríguez, Orbits in general relativity: the Jacobian elliptic functions, *Nuovo Cimento B* **98**(1), 87, 1987.
- [79] C. Miró Rodríguez, Unbound orbits in general relativity, *Nuovo Cimento B* **100**(6), 801, 1987.
- [80] A. F. Zakharov, Effective particle capture cross section of a Schwarzschild black hole, *Soviet Astronomy* **32**, 456 (1988).
- [81] A. F. Zakharov, Particle capture cross sections for a Reissner–Nordström black hole, *Classical and Quantum Gravity* **11**, 1027 (1994).
- [82] L. D. Landau and E. M. Lifshitz, *The classical theory of fields* (Pergamon, Oxford, 1993).
- [83] A. Accioly and S. Ragusa, Gravitational deflection of massive particles in classical and semiclassical general relativity, *Classical and Quantum Gravity* **19**, 5429 (2002).
- [84] O. Yu. Tsupko, Unbound motion of massive particles in the Schwarzschild metric: Analytical description in case of strong deflection, *Physical Review D* **89**, 084075 (2014).
- [85] X. Liu, N. Yang, and J. Jia, Gravitational lensing of massive particles in Schwarzschild gravity, *Classical and Quantum Gravity* **33**, 175014 (2016).
- [86] G. Crisnejo and E. Gallo, Weak lensing in a plasma medium and gravitational deflection of massive particles using the Gauss-Bonnet theorem. A unified treatment, *Physical Review D* **97**, 124016 (2018).
- [87] G. W. Gibbons and M. C. Werner, Applications of the Gauss–Bonnet theorem to gravitational lensing, *Classical and Quantum Gravity* **25**, 235009 (2008).
- [88] G. Crisnejo, E. Gallo, and K. Jusufi, Higher order corrections to deflection angle of massive particles and light rays in plasma media for stationary spacetimes using the Gauss-Bonnet theorem, *Phys. Rev. D* **100**, 104045 (2019).

- [89] X. Pang and J. Jia, Gravitational lensing of massive particles in Reissner–Nordström black hole spacetime, *Classical and Quantum Gravity* **36**, 065012 (2019).
- [90] G. He, X. Zhou, Z. Feng, X. Mu, H. Wang, W. Li, C. Pan, and W. Lin, Gravitational deflection of massive particles in Schwarzschild-de Sitter spacetime, *European Physical Journal C* **80**, 835 (2020).
- [91] T. C. Frost, Gravitational lensing of massive particles in the charged NUT spacetime, *Physical Review D* **108**, 124019 (2023).
- [92] K. Kobialko, I. Bogush, and D. Gal'tsov, Black hole shadows of massive particles and photons in plasma, *Physical Review D* **109**, 024060 (2024).
- [93] K. Kobialko and D. Gal'tsov, Perturbation theory for gravitational shadows in static spherically symmetric spacetimes, arXiv:2410.16127 (2024).
- [94] K. Kobialko, I. Bogush, and D. Gal'tsov, Geometry of massive particle surfaces, *Physical Review D* **106**, 084032 (2022).
- [95] I. Bogush, K. Kobialko, and D. Gal'tsov, Massive particle surfaces, *Physical Review D* **108**, 044070 (2023).
- [96] F. Feleppa, V. Bozza, and O. Yu. Tsupko, Strong deflection limit analysis of black hole lensing in inhomogeneous plasma, *Physical Review D* **110**, 064031 (2024).
- [97] R. Kulsrud and A. Loeb, Dynamics and gravitational interaction of waves in nonuniform media, *Physical Review D* **45**, 525 (1992).
- [98] A. Broderick and R. Blandford, Covariant magnetoionic theory – I. Ray propagation, *Monthly Notices of the Royal Astronomical Society* **342**, 1280 (2003).
- [99] G. S. Bisnovatyi-Kogan and O. Yu. Tsupko, Gravitational lensing in a non-uniform plasma, *Monthly Notices of the Royal Astronomical Society* **404**, 1790 (2010).
- [100] R. M. Quimby, M. C. Werner, M. Oguri, S. More, et al., Extraordinary magnification of the ordinary Type Ia supernova PS1-10afx, *The Astrophysical Journal* **768**, L20 (2013).
- [101] O. Mena, I. Mocioiu, and C. Quigg, Gravitational lensing of supernova neutrinos, *Astroparticle Physics* **28**, 348 (2007).
- [102] E. F. Eiroa and G. E. Romero, Gravitational lensing of transient neutrino sources by black holes, *Physics Letters B* **663**, 377 (2008).
- [103] J. L. Gerver, Focusing of neutrinos by the sun's core, *Physics Letters A* **127**, 301 (1988).
- [104] R. Escibano, J.-M. Frère, D. Monderen, and V. Van Elewyck, Insights on neutrino lensing, *Physics Letters B* **512**, 8 (2001).
- [105] X.-L. Luo, Neutrino lensing, *Chinese Physics Letters* **26**, 109801 (2009).
- [106] S. Adrián-Martínez, A. Albert, M. André, G. Anton, M. Ardid, J.-J. Aubert, B. Baret, J. Barrios-Martí, S. Basa, V. Bertin, et al., Constraining the neutrino emission of gravitationally lensed Flat-Spectrum Radio Quasars with ANTARES data, *Journal of Cosmology and Astroparticle Physics* **11** (2014) 017.
- [107] C. Corianò, A. Costantini, M. Dell'Atti, and L. D. Rose, Neutrino and photon lensing by black holes: radiative lens equations and post-Newtonian contributions, *Journal of High Energy Physics* **07** (2015) 160.
- [108] P. Amaro-Seoane, J. R. Gair, M. Freitag, M. C. Miller, I. Mandel, C. J. Cutler, and S. Babak, Topical review: Intermediate and extreme mass-ratio inspirals – astrophysics, science applications and detection using LISA, *Classical and Quantum Gravity* **24**, R113 (2007).
- [109] P. Amaro-Seoane, H. Audley, S. Babak, J. Baker, E. Barausse, P. Bender, E. Berti, P. Binetruy, M. Born, et al., Laser Interferometer Space Antenna, arXiv:1702.00786 (2017).
- [110] P. Amaro-Seoane, Relativistic dynamics and extreme mass ratio inspirals, *Living Reviews in Relativity* **21**, 4 (2018).
- [111] E. Hackmann and A. Dhani, The propagation delay in the timing of a pulsar orbiting a supermassive black hole, *General Relativity and Gravitation* **51**, 37 (2019).
- [112] B. Ben-Salem and E. Hackmann, Propagation time delay and frame dragging effects of lightlike geodesics in the timing of a pulsar orbiting SgrA*, *Monthly Notices of the Royal Astronomical Society* **516**, 1768 (2022).
- [113] M. P. Hobson, G. P. Efstathiou, and A. N. Lasenby, *General Relativity: An Introduction for Physicists* (Cambridge University Press, Cambridge, England, 2006).
- [114] K. S. Virbhadra, D. Narasimha, and S. M. Chitre, Role of the scalar field in gravitational lensing, *Astronomy and Astrophysics* **337**, 1 (1998).
- [115] P. I. Jefremov, O. Yu. Tsupko, G. S. Bisnovatyi-Kogan, Innermost stable circular orbits of spinning test particles in Schwarzschild and Kerr space-times, *Physical Review D* **91**, 124030 (2015).
- [116] V. Cardoso, A.S. Miranda, E. Berti, H. Witek, and V.T. Zanchin, Geodesic stability, Lyapunov exponents, and quasinormal modes, *Physical Review D* **79**, 064016 (2009).
- [117] H. Reissner, Über die Eigengravitation des elektrischen Feldes nach der Einsteinschen Theorie, *Annalen der Physik* **355**, 106 (1916).
- [118] G. Nordström, On the energy of the gravitational field in Einstein's theory, *Verhandelingen der Koninklijke Nederlandse Akademie van Wetenschappen, Afdeling Natuurkunde* **26**, 1201 (1918).
- [119] V. Perlick, O. Yu. Tsupko, and G. S. Bisnovatyi-Kogan, Influence of a plasma on the shadow of a spherically symmetric black hole, *Physical Review D* **92**, 104031 (2015).
- [120] I. Fisher, Scalar mesostatic field with regard for gravitational effects, *Zhurnal Eksperimental'noi i Teoreticheskoi Fiziki* **18**, 636 (1948).
- [121] A. I. Janis, E. T. Newman, and J. Winicour, Reality of the Schwarzschild singularity, *Physical Review Letters* **20**, 878 (1968).
- [122] M. Wyman, Static spherically symmetric scalar fields in general relativity, *Physical Review D* **24**, 839 (1981).
- [123] K. S. Virbhadra, Janis-Newman-Winicour and Wyman solutions are the same, *International Journal of Modern Physics A* **12**, 4831 (1997).
- [124] K. S. Virbhadra, S. Jhingan, and P. S. Joshi, Nature of singularity in Einstein-massless scalar theory, *International Journal of Modern Physics D* **06**, 357 (1997).
- [125] A. N. Chowdhury, M. Patil, D. Malafarina, and P. S. Joshi, Circular geodesics and accretion disks in the Janis-Newman-Winicour and gamma metric spacetimes, *Physical Review D* **85**, 104031 (2012).